

OLPT CONDUCTIVITY IN WOLLASTONITE INLAID NR/SBR TYPE ELASTOMER BASED MATERIAL

#E. ŞENTÜRK, T. YÜKSEL, M. OKUTAN*, A. DEMIRER**, N. AKÇAKALE***, İ. OKUR

Department of Physics, Sakarya University, Esentepe Kampus, Sakarya, Turkey

**Department of Physics, Yıldız Technical University, Istanbul, Turkey*

***Department of Machine Education, Sakarya University, Esentepe Kampus, Sakarya, Turkey*

****Department of Computer Technologies, Abant İzzet Baysal University, Bolu, Turkey*

E-mail: senturk@sakarya.edu.tr

Submitted January 27, 2012; accepted May 6, 2012

Keywords: Polymers, Electrical properties, Polymer-matrix composites (PMCs), Thermal properties

The electrical properties of wollastonite inlaid NR/SBR type elastomer based material have been evaluated. Electrical properties of the samples were measured in the temperature range of 303 to 453 K and the frequency range of 100 Hz – 40 MHz. All electrically measured parameters were given anomalies at 385 K. Only one type of dielectric relaxation process have been observed for all measurements. Physical parameters characterizing the dielectric behavior have been obtained by fitting the experimental results in the modified Debye equation. The activation energy which is thermally activated by dielectric relaxation process have been calculated to be 0.58 eV. DC conductivity increasing by temperature has been explained with the help of VFT model whereas the AC one has been clarified by the OLPT model.

INTRODUCTION

Natural rubber/Stiren Butadien rubber (NR/SBR) type elastomers obtained by mixing natural and synthetic rubbers in proper ratio are of importance nowadays since they exhibit unique properties especially in the industrial processes. Automotive, construction, household appliances and shoes base materials are some of the examples for these types of elastomers. Especially in the shoes industry, 34% of the rubber base materials are of this type [1-2]. The products of this type might be inlaid with various materials so that they might have been processed in any way at the end of the producer point.

In previous studies [3, 4, 5, 6, 7], for elastomers, glass fiber, wood powder, leather powder, glass balls, rice husk, mica powder and wollastonite were used as additives for the elastomers as well as the conventional fillet materials.

The mechanical and physical property changes of SBS block copolymers by inlaying 10 % mica and 10 % small glass balls rather than calcium carbonate (CaCO_3) into the structure for the rheological behaviours of the shoes base materials' dopants have been studied [3]. Since silicon is not cheap material compared to the other inlays of mica powder and calcium carbonate, it will cost much so that the mica powder seems to be a good candidate for these kind of processes. The mechanical properties

of NR/SBR type elastomer based materials inlaid mica powder in three different ratios were studied [8]. In this work, they used mica powder (SMW 375) inlays 5.15 %, 9.4 % and 13.4 %, which is 250, 500 and 750 grams in weight, respectively and they observed an increase of 16.5 % in expansion and increase of 36 % in tensile strength. Small amount of increase in wearing rate was also noticed whereas the stiffness was observed within the expected ranges. Material unit cost was detected to decrease about 5.2-12 %.

In elastomer materials, glass powder inlays eases the electrical conduction, wood chips decrease the costs, aluminium powder strengthens the mechanical toughness, and paper chips and cloth powders provide good insulation [4].

In triple mixture of polypropylene/ethylene-propylene-dien terpolymer/white brass crust powder thermoplastic elastomers, it has been found that this PP/EPDM/White brass crust decreases the product deformation in rubbers. Furthermore, this mixture increases the materials viscosity and melting viscosity to some extent and 4 % inlaid specimen shows dead flat surface structures [5].

The compressive, tensile and impact strength values after adding 2-10 % of peanut crust powder to polyurethane were measured. In this study, it was pointed out that the inlays had negative effect on the impact strength. The optimal case was observed for the tensile

strength in the 4 % rate whereas the worst was seen in the case of 8 %. They concluded from their research that this inlay, i.e. peanut curst powder, might be used in polyurethane products [9].

The mechanical characteristics of elastomer materials obtained by inlaying wollastonit in 5.15 %, 9.4 % and 13.4 % have shown higher buckling capacity than the standard values and the stretching amount was to be 13 % higher than the normal ones and this gave 11 % progress in total efficiency. It was declared that there exists 13.4 % to 41% increase in tensile (breaking) strength. Increase in wollastonite rate in elastomer rose the wearing and stiffness values to some extent and this decreased the product unit cost about 5.7-12 % [11]. The use of small grain sized carbon blacks as inlays had an effect of increasing tearing and wearing strength of natural rubbers [11].

Dielectric analysis method was used in characterizing the electrical properties of various type samples within a large frequency range. In polymers, both molecular dynamics and conduction mechanisms are the general topics for this method. In the current work, it was aimed at finding out the electrical properties, rather than mechanical ones, of wollastonite inlayed NR/SBR type elastomer material with respect to the temperature which were higher than the room temperature.

EXPERIMENTAL

NR/SBR type elastomer based material is a mixture of natural (NR RSS3) and Stiren Butadien (SBR 1502) rubber. To increase the elasticity, smoothness and strengths, eight different inlays and wollastonite (W) 5.15 % rates in weight, were added to obtain elastomer mixture.

Wollastonite is a mineral of calcium silicate (CaSiO_3) produced in the contact process of acid intrusive and limestone. In its pure state its color is white and it shows fiber structure. Its color can be changed to brownish to dark grey, depending on the impurities added in. Its advantages in energy savings as well as

showing small volume shrinking after annealing, high mechanical strength, controllable porosity and better isolation characteristics determine its area of usage. Due to its unique characteristics it is being used in ground and wall tiles and singly cooked glazed tile productions as well as in electrical isolators, porcelains, vitrifies, enamels, mineral fibers, white paints and abrasive disk production.

Since carbon black HAF N330, which are used in mixtures as active filling agent, has smaller grain sizes, it makes the structure more homogeneous. Clear colored petroleum jelly as softener, stearic acid and zinc active dopants as activators were added to the dough. Rubbers and added materials content rates used in the experiments are listed in the Table 1.

In the experimental procedure, after preparing rubber dough inlayed with wollastonite it was subjected to the vulcanization process. Care has been taken to arrange the same experimental conditions in both the preparation of the dough in banbury and cooking them in the hot press. Mixtures prepared in special Rolling cyllinders as plates were vulcanized in vulcanizing press under temperature control and of 160 atm pressure and transformed to the sheets.

First of all the samples were cut in the dimension of ~ 20 mm in radius and ~ 5 mm in width. Then its both faces were grinded and all surfaces were made to be flat. After that the sample's width, radius and surface area were measured to be used in the calculation of the real and imaginary part of the dielectric constant and conductivity. Top and bottom faces of the specimen were coated with silver dag to have electrical conductivity and then it left to be dried.

Before the measurements the calibration were performed for the HP 4194 A Impedance-Gain/Phase analyzer. After the calibration the sample was placed to the furnace. Electrical capacitance and conductivity measurements were fulfilled simultaneously. Data were taken in the frequency interval of 100 Hz to 10 MHz and for the temperatures from 303 to 453 K. All measurements were recorded for the logarithmically arranged 26 different frequency points. Data taking process took the time less than a couple of seconds and a Bias voltage of less than 1 V was applied during the process to get the dipol orientation. HP 4194 A Impedance-Gain/Phase analyzer and temperature control unit as well as the furnace were being monitored and controlled by a special computer software. The measurement results have been displayed in the screen of HP 4194 A Impedance-Gain/Phase analyzer and in the computer screen simultaneously and the data have been saved for the further use.

RESULTS AND DISCUSSION

Figure 1 shows temperature and frequency dependency of the real part of the dielectric constant of the sample. As can be seen from the figure the real part

Table 1. The rubbers and inlay matters ratios used in the experiments [1].

Components	(%)
NR+SBR	11.2 + 33.4 = 44.6
Carbon black, HAF N330	29.7
Wollastonite	5.15
Sulphur	1.35
Active zinc	1.5
Stearic acid	0.9
Paraffinic oil	5.9
Silicasyl	10
Vulcanization accelerators (CZ, TH, DEG, MBT)	1.4

of the dielectric constant is ultimately dependent on both the temperature and the frequency. Increasing the temperature raises the dielectric constant progressively and it reaches to a maximum at about 385 K. The position of this peak shifts curly to the lower temperatures for the higher frequencies. For the higher temperatures molecular mass loss occurs naturally. Due to this loss, the segmental movement of the molecular chain, which has bigger mass close to the room temperature, slows down. This means that in the lower temperatures this movement needs higher frequencies for the energy demand. For the higher temperatures, decreasing molecular mass urges less energy and this causes the placement of the phase transition temperature to locate at the lowered frequency values. This peak probably stands for a phase transition.

Furthermore, peak intensity decreases by increasing the frequency. This behaviour can be explained by the fact that the electric dipoles behave slower than the rate of the applied field and thus the polarization cannot respond to the field. Even though the real part of the dielectric constant changes to some extent at the frequency of 5.42 kHz, it does not change much at the higher frequency values and it becomes frequency and temperature independent if the flat region is monitored carefully. However, there exists an interesting profile here that a small change in the electric field induces a rapid decrease in the peak intensity of the dielectric constant. This behaviour can be attributed to that the long chained molecular structure cannot respond to the field simultaneously and there may be an effective conductivity during the process.

In addition to these, the rate of decrease for the dielectric constant is much slower in the higher temperatures than that in the lower ones. This implies different conductivity effects originated by the two distinct

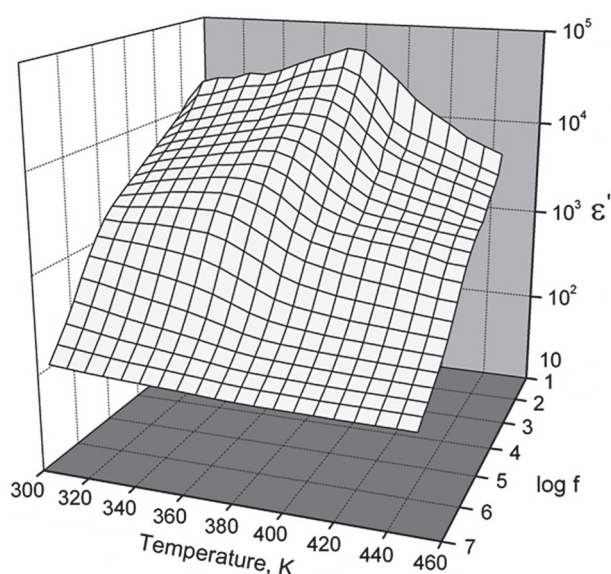


Figure 1. Temperature and frequency dependencies of the real part of dielectric constant.

structures by possible phase transitions. Furthermore, this is a clear evidence that in the temperature interval dielectric relaxation as well as the conductivity occurs rapidly for the lower temperatures whereas it happens slowly for the higher temperatures.

The values of dielectric constant at the lower frequencies are denoted to be ϵ_0 for $\lim_{\omega \rightarrow 0} \epsilon'(\omega)$. This is called static dielectric constant. For the higher frequency region at which the flat style behaviour of the dielectric constant is dominated, the value of ϵ_∞ for $\lim_{\omega \rightarrow \infty} \epsilon'(\omega)$ is called dynamic dielectric constant. The difference of these two, i.e. $\Delta\epsilon = \epsilon_0 - \epsilon_\infty$, is termed dielectric strength. As can be seen both from the Table 2 and Figure 1, the real part of the dielectric constant clearly increases up to possible phase transition temperature by raising the temperature and then lowers down. As a result of this behaviour, it can be said that the dielectric strength increases by increasing the temperature up to possible phase transition and then decreases gradually. In contrast to that, dynamic dielectric constant stays stable at about 20 for all temperatures and higher frequencies. This is attributed to the slow motion of the electric dipoles which cannot respond to the electric field applied. At the lower and higher frequencies dielectric intensity is expressed as [12]

$$\frac{\Delta\epsilon(2\Delta\epsilon + 3\epsilon_\infty)}{(\Delta\epsilon + 3\epsilon_\infty)} = \frac{4\pi g N \mu}{9k_B T \epsilon_v} \quad (1)$$

where k_B is Boltzmann constant, T is absolute temperature, N is the concentration of dipoles, μ is the dipole moment of the polymer chain and ϵ_v is vacuum dielectric constant and g is a correlation factor which is in general equal to 1.

From Figure 1 such a relaxation process can be seen at the frequency of about 10^5 Hz. This relaxation has been interpreted as dipolar type relaxation in frequency caused by the longer chains in the polymer materials.

For the curvature centers obtained from the variation of the real part of the dielectric constant with respect to the imaginary one to stay on about the real axis, relaxation distribution parameters in Havriliak-Negami equation have to be taken equal to 1 [13]. Therefore, this approximation converts the present model to simpler Debye model. Debye model assumes that the drawn curves relevant to the real and imaginary part stay exactly on the horizontal axis. According to the model, dipoles contributing to the dielectric constant do not interact with each other.

However, both real and imaginary parts of the dielectric constants cannot be represented thoroughly with this model since experimental results show remarkable deviation from the Debye model, especially in the lower frequencies. This effect can be seen in the Figure 1, in the lower frequency values the real part of the dielectric constant deviate rapidly especially in the phase transition region whereas it occurs slowly in the lower temperatures. This behaviour is different from

that of the conventional Debye model presumes. To make an accurate analysis in this frequency region for the dielectric behaviour one may assume the effect of conductivity. Therefore, in addition to the Debye model the variation of the real part of the dielectric constant with respect to the frequency may be represented with this conductivity contribution [14]. Thus, the modified Debye model consists of two terms [13]

$$\epsilon'(w) = \epsilon_\infty + \frac{\epsilon_o - \epsilon_\infty}{1 + w^2 \tau^2} + \frac{\sigma_o}{\epsilon_v} w^{-s} \cos\left(\frac{\pi s}{2}\right) \quad (2)$$

where w is angular frequency, s is the power parameter (between 0 to 1) representing the variation of conductivity with respect to frequency, σ_o is DC conductivity and τ is the relaxation time. Each experimental values of the sample regarding to the variation of the real part of the dielectric constant with respect to the frequency for all temperatures were fitted to the equation 2.

Figure 2 shows the variation of the imaginary part of the dielectric constant with respect to the frequency in various temperatures. As in real part, the imaginary

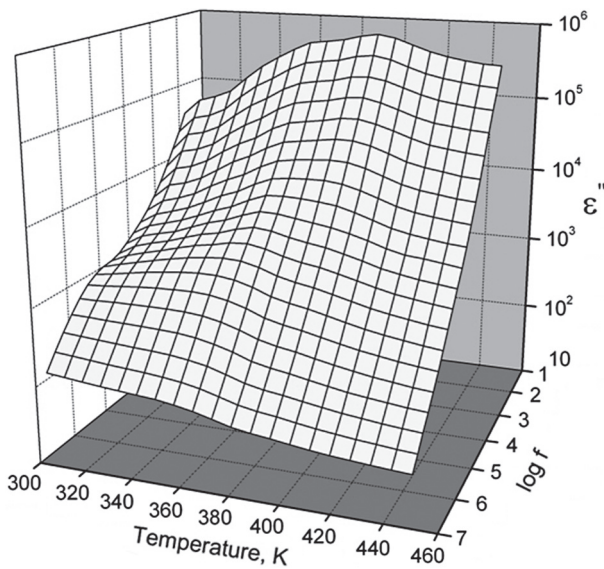


Figure 2. Temperature and frequency dependencies of the imaginary part of dielectric constant.

part clearly exhibits temperature and frequency dependencies. It is well known that the imaginary part emerges as a measure of the loss of the externally applied field's energy to the sample. From the figure it can be seen that the imaginary part has higher values and decreases rapidly with increasing frequencies. This behaviour can be interpreted as a result of the ionic conductivity occurred in the polymers. In addition to this the phase transition peak set by the real part in the critical temperature appears here again for the imaginary part at about 385 K.

As can be seen from the figure, the imaginary part decreases with increasing frequencies. As is the case for the real part, rapid variation for the imaginary part with increasing frequency occurs in the phase transition region. This shows that the rapid and smooth decrease in lower frequency is dominated in this region. From this result one may interpret that the conductivity contribution is likely here for the imaginary part as is the case for the real part. Conductivity behaviour represented by the linear decrease especially in the higher temperatures dominates the imaginary peak which is a measure of the dielectric loss and characterizing the dielectric relaxation. However, this is not valid for the temperature region of 303 to 343 K. Except this region, conductivity dominates the loss peak throughout the all temperatures and frequencies. The relaxation occurring at $\sim 10^5$ Hz for the real part stands for at the temperatures at which the conductivity does not dominate. However, for the lower temperatures it can be said that the increasing temperature shifts the relaxation frequencies towards the lower ones. This implies that the relaxation takes longer time as temperature is increased. In the light of these discussions, we may conclude that we need to add a conductivity term for the imaginary part as well. In this case, modified model for the imaginary part becomes [13]

$$\epsilon''(w) = (\epsilon_o - \epsilon_\infty) \frac{w\tau}{1 + w^2 \tau^2} + \frac{\sigma_o}{\epsilon_v} w^{-s} \sin\left(\frac{\pi s}{2}\right) \quad (3)$$

Fitted values of experimental results according to the last equations are given in Table 2. Fitting has been simultaneously performed for both the real and the imaginary parts. It has been shown that there exists a good

Table 2. The results gained by fitting the experimental data to the theory.

	ϵ_o	ϵ_∞	$\sigma (Sm^{-1})$	s	$\tau (s)$	$\epsilon_o - \epsilon_\infty$
303 K	1350	10	0.00000250	0.43	0.00000046	1340
323 K	1720	13	0.00000205	0.42	0.00000090	1707
343 K	3000	10	0.00000170	0.41	0.00000175	2990
363 K	3000	10	0.00000140	0.41	0.00000250	2990
383 K	4500	10	0.00000160	0.42	0.00001400	4490
403 K	2700	10	0.00000200	0.44	0.00004500	2690
423 K	1800	20	0.00000250	0.46	0.00006000	1780
443 K	1400	35	0.00000260	0.47	0.00015000	1365

agreement between the experimental and theoretical values for the both part of the dielectric constant.

Figure 3 shows the variation of the dielectric relaxation time with respect to the temperature. This variation infers a thermally activated relaxation process. The variation of the relaxation time with respect to temperature is given by [15]

$$\tau = \tau_0 \exp\left(-\frac{E_a}{k_B T}\right) \quad (4)$$

where τ_0 is a pre-exponential factor and E_a is an activa-

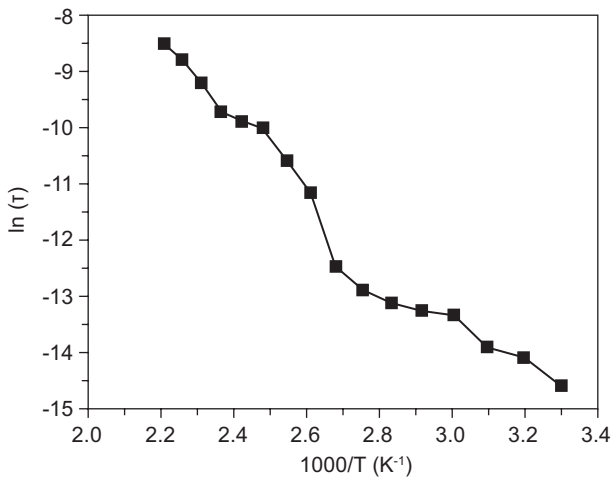


Figure 3. Relaxation time-temperature relation.

tion energy. Fitting the experimental curve to this equation gives the activation energy to be 0.58 eV.

As can be seen from Figure 4, dependence of imaginary part with respect to real part shows a single relaxation mechanism. At some temperatures, it can be concluded that there exists both uncompleted semi-

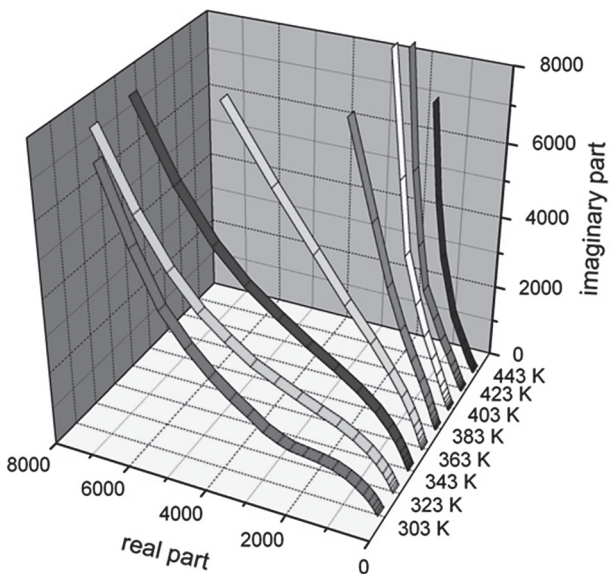


Figure 4. Variation of imaginary part of dielectric constant with respect to real part at different temperatures.

circles and uncleared circles. This is especially the case for the temperatures of 303-343 K. However, another behaviour of dominating conductivity effect is also in progress especially in the right hand side of this curve which is in the lower frequency region and decreasing abruptly from a very high value. This behaviour seems to have similar results for both the real and imaginary parts' frequency variation curves. However this result does not mean that such a mechanism is absent for these temperatures. It can be deduced only that the present conductivity effect is appeared at these temperatures and that the relaxation mechanism becomes dominant.

The curves deducible from the incomplete curves for the lower temperatures form a thorough-semi circle and the focus of the circle stays on the real axis. As stated above that the present experimental results might be handled with the Havrilak-Negami model modified to the Debye model. The model has been therefore converted to a form containing the electrical conductivity representing the lower frequency behaviours. The force parameter values in Havrilak-Negami model were set equal to 1 to transform to this model and this was in good accordance with the symmetry of the curves.

Figure 5 shows the variation of conductivity with respect to temperature and frequency. Conductivity takes the values of 10^{-6} to 10^{-3} S/cm in the temperature and frequency interval. As the mobility of the ions is slower in these temperature and frequency values, the conductivity of the sample can be said to be in the ionic conductivity form [16]. As can be easily seen from the figure, the conductivity is strongly dependent upon both the temperature and the applied AC field frequency. Conductivity consists of two distinct regions for all temperatures.

The first region is the DC conductivity region in which the conductivity is constant for the lower frequen-

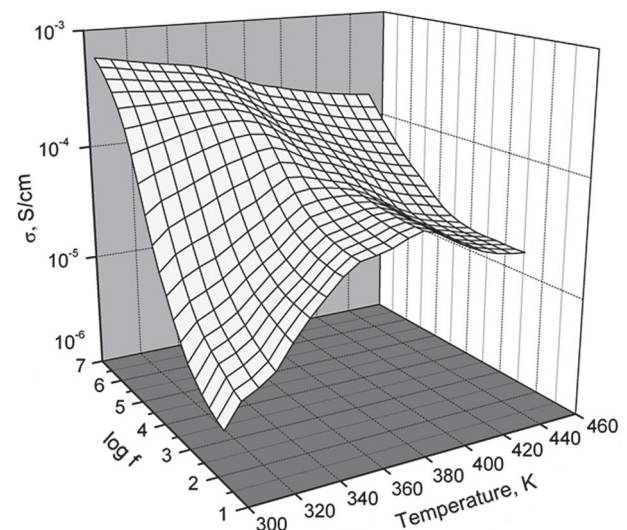


Figure 5. Temperature and frequency dependency of conductivity at various temperatures.

cies. For the temperatures which are higher than the phase transition temperatures the conductivity is fixed and this is seen as a plateau in the figure. In the second region conductivity increases rapidly with increasing frequency and this area is called AC conductivity region. This behaviour is very clear especially for the lower temperatures. It can be concluded that the AC conductivity dominates in higher frequencies as more and more ions displace so that more ions in unit volume in this frequency region contributes to the conductivity by hopping process. This experimental behaviour can be represented by the universal Jonscher law which is a sum of conductivity terms in which the terms initially stays stable and then increases rapidly with frequency [17]

$$\sigma(\omega) = \sigma_o + A\omega^{s(T)} \quad (5)$$

Temperature dependency of s values fitted to the Equation (5) for all temperatures is shown in Figure 6. The power parameter initially decreases and then increases via temperature. The variation of s parameter of conductivity with respect to the temperature reveals the

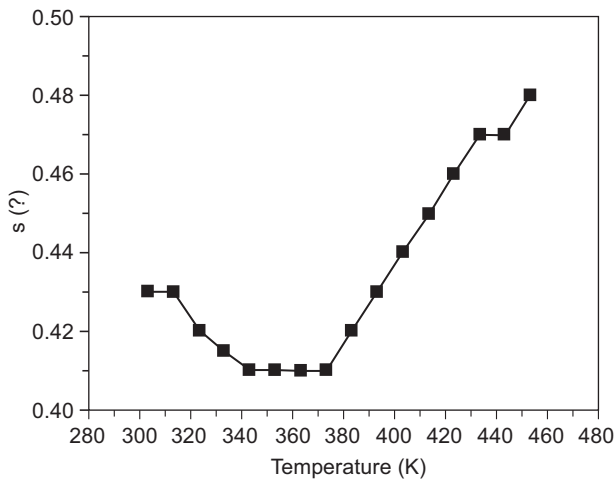


Figure 6. Variation of s parameter by temperature.

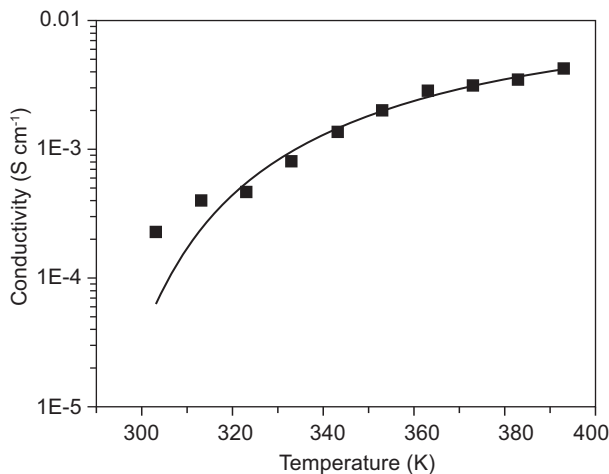


Figure 7. Variation of DC conductivity with respect to the temperature.

type of conductivity of the sample. From the tendency of this parameter to go initially down producing a minimum and then to rise up to a top value, one can conclude that the conductivity can be explained by the overlapping large polaron tunneling (OLPT) model [18, 19]. However, the variation rate of conductivity by frequency in higher temperatures seems to be slower than the lower temperatures. In fact, this strange (fast and slow) variation of conductivity characterizes the likely phase transition which is assumed to be occurred at 385 K.

Figure 7 depicts the variation of conductivity versus temperature. The close dependency is clearly seen in this graph as well. Increasing temperature raises the conductivity to some extent. From the flat region of AC conductivity in lower frequencies the variation of DC conductivity of the sample has been attained. Relatively curved DC conductivity behaviour with respect to temperature is conventional for the polymers exhibiting ionic conductivity [20]. Increasing conductivity by the increase of the temperature can be explained by the free volume model. In this process, to increase the temperature causes the polymers to expand in volume and this creates free spaces. These free spaces becomes bigger and bigger as temperature rises up to higher degrees. To comment on the sample's temperature behaviour on the conductivity this effect is taken into account. As temperature raises up, both ions which are likely to contribute to conductivity, polymer segments and decomposed molecules move around and elevate the conductivity to higher values as can be seen in Figure 5 [21].

This temperature dependent behaviour does not fit the classical Arrhenius profile in logarithmic scale and it wanders from the line in higher temperatures. This type of conductivity behaviour relates with the equation [22, 23]

$$\sigma(T) = KT^{-0.5} \exp \left[\frac{-E_p}{k_B(T-T_o)} \right] \quad (6)$$

This relation is known as Vogel-Fulcer-Tamman (VFT) formula where E_p is pseudoactivation energy for the ionic conductivity, K is an pre-exponential factor related to the charge carriers and T_o is called semi-equilibrium glass transition temperature. It is a limiting value up which no entropy changes occur due to the configuration variation [23]. The dots in the Figure 7 denote the experimental values whereas the solid line is a fit for these data. The value of T_o is 30 to 50 °C lower than the glass transition temperature [22]. Taking these parameters to be 0.18 eV, 0.43 S cm⁻¹ and 268 K fits the solid line best to the experimental values.

CONCLUSIONS

It has been found that both the real and imaginary part of the dielectric constant lowered down by

increasing frequencies. Both temperature and frequency dependencies of the real and imaginary part of the dielectric constant, dielectric intensity and s parameter showed a variation at 385 K. The real and the imaginary part exhibited abrupt declines especially in the lower frequency region. These variations have been evaluated according to the Debye model, attributing the variations to conductivity. At the temperature values which were higher than the critical phase transition temperature, loss peak diminished. This can be interpreted as that the conductivity dominated the imaginary part of dielectric constant.

For the inspected temperatures, both the variation of the real and the imaginary part with respect to frequency and the variation of the real part with respect to the imaginary part implied a single dielectric relaxation process. This process was tried to be explained in the light of the modified Debye model and the results which were obtained by fitting the experimental data to the theoretical model were given in Table 2. From this fitting process and the relaxation time, the activation energy was found to be 0.58 eV.

From the experimental results it has been observed that the conductivity initially stayed stable and then gradually increased to some extent. Frequency independent DC conductivity has been explained by using VFT model. Increasing DC conductivity with temperature has been found to be considered employing ionic conductivity and that the glassy matrix was observed to be dispersed in a large temperature interval, i.e. larger than the conventional temperature intervals, so that the conductivity was increased up to higher temperature values. AC conductivity mechanism at higher frequencies characterized by s parameter was found to be OLPT type.

References

1. Warrington S., Rubber N.: Footwear Open Tech, Satra Footwear Technology Center, Module 31, London, 1994.
2. Akçakale N., Demirer A., Özsert I.: Investigation of The Effect of Some Addives on The Mechanical Properties of NR/SBR Elastomer Based Sole Materials, Sakarya University Intitute of Science, Sakarya 2008.
3. Jolene F. S., Nunes R. C. R., Pita V. J.: Rheological Behavior of Mineral Fillers in Shoe Soles Composites, Universidade Federal do Rio de Janeiro P.O Box 68525 Rio de Janeiro, RJ, Brazil, 2000.
4. Timings R. L.: Materials Technology Level 3 1. Materials Science, Longman House Burnt Mill, Hartow Essex CM20 2ZJ, England 1985.
5. Siriwardena S., Ismail, H., Ishiaku U.S.: The Effect of Filler Loading And Curing Agent Concentration On Rheological Properties of Polypropylene/Ethylene-Propylene-Diene-Terpolymer/With Rice Husk Ash Thermoplastic Elastomer Ternary Composites, School of Materials and Mineral Resources Engineering, University Sains, Malaysia, 2001.
6. Oksman K., Crain C.: Journal of Applied Polymer Science 67, 101 (1988).
7. Sumaila M., Ugheoke B.I., Timon L., Oloyede T.: A Preliminary Mechanical Characterization of Polyurethane Filled with Lignocellulosic Materials, Federal University of Technology, Yola, Nigeria 2001.
8. Demirer A., Özsert I.: Investigation of The Effect of Mica Powder on The Mechanical Properties of NR/SBR Based Elastomer Material, 5. International Advanced Technologies Symposium (IA TS'09), 13-15 May. 2009, Karabuk, Turkey.
9. Ichazo M.N., Hernandez M., Albano C., Gonzales J.: Proceeding of the 8th Polymers of Advanced Technologies International Symposium, Budapest, Hungary 2005.
10. Akçakale N., Demirer A., Nart E., Özsert I.: Scientific Research and Essays 5, 758 (2010).
11. Savran, Ö. H.: Elastomer Technologies 1-2, Publication of Rubber Association, Istanbul, Türkiye, 2001.
12. Ryabov Y. E., Marom. G., Feldman. Y., Journal of Thermoplastic Composite Materials, 17, 463 (2004).
13. Raissi T., Ramdani N., Ibos L., Candau Y.: Proceedings of the 5th International Conference on Inverse Problems in Engineering: Theory and Practice, Cambridge, UK , 11-15th July 2005 .
14. Karan N.K., Pradhan D.K., Thomas R., Natesan B., Katiyar R. S., Solids State Ionics 179, 689 (2008).
15. Gamal Sobhai Said, Fawazy Hamed Abd-El Kader, Mohamed Mahross El Naggar, Badawi Ali Anees, Carbohydrate Polymers 65, 253 (2006).
16. Kato Y., Hasumi K., Yokoyama S., Yabe T., Ikuta H., Uchimoto Y., Wakihara M.: Solid State Ionics 150, 355 (2002).
17. Reda S.M.: Dyes and Pigments 75, 526 (2007).
18. Afifi M.A., Bekheet A.E., Abd Elwahhab E., Atyia H.E.: Vacuum 61, 9 (2001).
19. Okutan M., Basaran E., Halil I.B., Yakuphanoglu F.: Physica B 364, 300 (2005).
20. Karan N. K., Pradhan D. K., Thomas. R., Natesan B., Katiyar R. S.: Solids State Ionics 150, 355 (2002).
21. Saikia D., Chen-Yang Y. W., Li. Y. T., Lin. S. I.: Desalination 234, 24 (2008).
22. Xiping H., Kok S.S.: Polymer 41, 8689 (2000).
23. Liming D.: Polymer 38, 4267 (1997)